Acta Crystallographica Section F
Structural Biology and Crystallization Communications
ISSN 1744-3091

Crystallization and preliminary X-ray diffraction studies of the (*R*)-selective amine transaminase from *Aspergillus fumigatus*

Maren Thomsen,‡ Lilly Skalden,‡ Gottfried J. Palm, Matthias Höhne, Uwe T. Bornscheuer and Winfried Hinrichs*

Institut für Biochemie, Universität Greifswald, Felix-Hausdorff-Strasse 4, D-17489 Greifswald, Germany

‡ These authors contributed equally to this work.

Correspondence e-mail: winfried.hinrichs@uni-greifswald.de

Received 4 October 2013
Accepted 11 November 2013

The (*R*)-selective amine transaminase from *Aspergillus fumigatus* was expressed in *Escherichia coli* and purified to homogeneity. Bright yellow crystals appeared while storing the concentrated solution in the refrigerator and belonged to space group $C222_1$. X-ray diffraction data were collected to 1.27 Å resolution, as well as an anomalous data set to 1.84 Å resolution that was suitable for S-SAD phasing.

1. Introduction

Transaminases belong to the pyridoxal-5′-phosphate (PLP)-dependent enzymes and catalyze the reversible transfer of an amino group to an α-keto acid, ketone or aldehyde (Hayashi, 1995). The PLP and the catalytic lysine side chain are the key elements in this reaction (Eliot & Kirsch, 2004).

Transaminases are of biotechnological significance because of their ability to produce enantiopure amines from prochiral precursors. These amines are applied as ingredients or synthons in medicine, agrochemistry, pharmacy and chemistry (Merck, 2001; Deng *et al.*, 1995; Martens *et al.*, 1986; Höhne & Bornscheuer, 2009).

Based on their substrate range, transaminases can be divided into α-transaminases, ω-transaminases and amine transaminases. Whereas the substrates of α-transaminases require a carboxylate in the α position, the substrates of ω-transaminases have up to five extra C atoms between the terminal amino function and the carboxylate. The substrates of amine transaminases can lack the carboxyl group completely (Höhne & Bornscheuer, 2012; Mani Tripathi & Ramachandran, 2006). Amine transaminases often show excellent enantioselectivity and can be grouped into two classes. (*R*)-Amines are generated by (*R*)-selective amine transaminases when the quinoid intermediate of the reaction is protonated from the catalytic lysine at the *si*-site (Hanson, 1966). Alternatively, the (*S*)-amine is produced by an (*S*)-amine transaminase when the protonation occurs at the *re*-site.

Aspergillus fumigatus is a mildew which can cause respiratory allergy. It is a thermophilic saprophytic fungus with a worldwide distribution (Latgé, 1999). The sequence of an (*R*)-selective amine transaminase from *A. fumigatus* was identified by an *in silico* search (Höhne *et al.*, 2010) and is available online at NCBI (NCBI Reference Sequence XP_748821.1).

Several structures of α-transaminases have been described and these enzymes have been studied in detail (Schwarzenbacher *et al.*, 2004; Han *et al.*, 2006). Recently, a few crystal structures of non-homologous (*S*)-selective amine transaminases have been published (Steffen-Munsberg *et al.*, 2013; Humble *et al.*, 2012). In contrast, only a homology model of an (*R*)-selective amine transaminase from an *Arthrobacter* species based on a D-amino-acid aminotransferase (PDB entry 3daa) has been published (Savile *et al.*, 2010). Here, we describe expression, purification, crystallization and initial crystallographic results to elucidate the structure of the (*R*)-selective amine transaminase (AspFum) from *A. fumigatus*.

2. Materials and methods

2.1. Protein expression and purification

The gene for the amine transaminase was expressed in *Escherichia coli* BL21 (DE3) cells containing the expression vector pET-22b, which encodes the sequence of the amine transaminase including an additional C-terminal His_6 tag (SGSHHHHHH; Höhne *et al.*, 2010). The recombinant protein consists of 332 amino-acid residues with a molecular weight of 37.16 kDa. The cells were grown at 310 K in 400 ml LB medium containing 0.1 mg ml^{-1} ampicillin until an OD_{600} of 0.4 was reached. The temperature was then reduced to the expression temperature of 293 K and the cells were further incubated until they reached an OD_{600} of 0.7. Expression of the protein was induced by the addition of 1 m*M* IPTG. The cells were harvested 20 h after induction (Höhne *et al.*, 2010).

The cell pellet was resuspended in 50 m*M* sodium phosphate buffer pH 7.5, 300 m*M* sodium chloride (buffer *A*) containing an additional 0.1 m*M* PLP and 30 m*M* imidazole. Cell disruption was performed by two passages through a French press at 10.3 MPa. The resulting suspension was centrifuged for 45 min at 10 000*g*. The filtrated supernatant was applied onto a nickel–NTA column (GE Healthcare). After washing with three column volumes of buffer *A* containing 60 m*M* imidazole at a flow rate of 5 ml min^{-1}, the protein was eluted with buffer *A* containing 300 m*M* imidazole. The amine transaminase-containing fractions were identified using an acetophenone assay (Schätzle *et al.*, 2009), collected and pooled. The pooled protein was then desalted by gel chromatography against 20 m*M* tricine buffer pH 7.5, 10 µ*M* PLP at a flow rate of 2 ml min^{-1} (Höhne *et al.*, 2010). The desired concentration of AspFum was achieved by ultrafiltration with Vivaspin 6 columns (molecular-weight cutoff 10 kDa; Sartorius Stedim).

2.2. Crystallization

Initial crystallization hits were obtained with a variety of PEG-based conditions (JBScreen Classic 1–10, Jena Bioscience) within 4 d. However, all diffraction images of these crystals were not indexable. Suitable crystals of AspFum appeared after six months in an Eppendorf reaction tube containing concentrated protein (10.7 mg ml^{-1}) and 20 m*M* tricine pH 7.5 with 10 µ*M* PLP at 277 K.

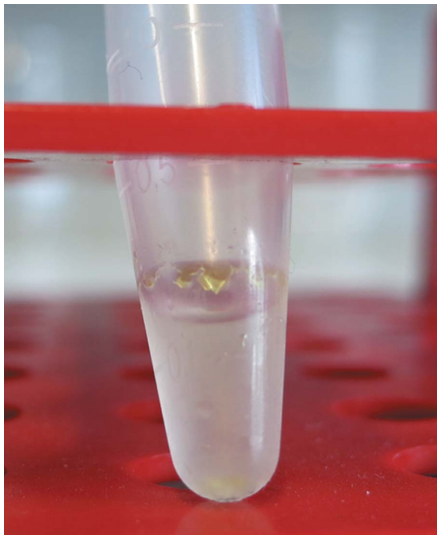

Figure 1
Crystals of the (*R*)-selective amine transaminase from *A. fumigatus* grown in an Eppendorf reaction tube.

Table 1
Data-collection and processing statistics.

Values in parentheses are for the outermost resolution shell.

Data set	Native	Anomalous
Beamline	14.1, BESSY II	14.1, BESSY II
Detector	Pilatus 6M	Pilatus 6M
Wavelength (Å)	0.91841	1.77122
Temperature (K)	100	100
Orthorhombic space group	$C222_1$	$C222_1$
Unit-cell parameters (Å)	a = 102.2, b = 120.9, c = 135.4	a = 102.2, b = 120.9, c = 135.4
Resolution range (Å)	50.0–1.27 (1.35–1.27)	50.0–1.84 (1.95–1.84)
No. of unique reflections	426722 (68273)	135117 (17260)
Multiplicity	3.38 (3.3)	5.6 (2.6)
R_{merge} (%)	6.3 (60.3)	3.9 (9.5)
Mean $I/\sigma(I)$	13.2 (2.0)	30.29 (8.34)
$CC_{1/2}$† (%)	99.9 (73.0)	99.9 (98.8)
Completeness (%)	99.1 (97.9)	95.9 (75.8)
Overall B factor from Wilson plot (Å^2)	17.4	18.8
Total rotation, increment (°)	180, 0.1	360, 0.1

† $CC_{1/2}$ is the percentage correlation between intensities from random half data sets (Karplus & Diederichs, 2012).

The crystals could easily be seen by eye (>1 mm) and had a very bright yellow colour, suggesting bound PLP (Fig. 1). Only the small crystals (<0.4 mm) present at the bottom of the tube diffracted to high resolution. The mechanical stress on the large crystals attached to the wall of the reaction tube while fishing and upon cooling led to loss of diffraction quality.

2.3. Data collection and X-ray crystallographic analysis

For cryoprotection, a solution consisting of 35%(*v*/*v*) glycerol, 20 m*M* tricine pH 7.5, 10 µ*M* PLP was used. X-ray diffraction data were collected at 100 K on beamline 14.1 at the BESSY II synchrotron source, Berlin, Germany (Mueller *et al.*, 2012). Two data sets were collected from one crystal. The first was collected at a wavelength of 0.9184 Å using the highest intensity and the second was collected at 1.77 Å to obtain a large anomalous signal from the S atoms present in the protein. The resolution range of the anomalous data set was limited by the detector geometry. All diffraction images were processed with *XDS* (Kabsch, 2010) using the graphical user interface *XDSapp* (Krug *et al.*, 2012). The rotation function was calculated using *MOLREP* (Vagin & Teplyakov, 2010; Winn *et al.*, 2011) with a resolution range of 30–3 Å and a radius of integration of 30 Å. Data-collection and processing statistics are given in Table 1.

3. Results and discussion

The (*R*)-selective amine transaminase from *A. fumigatus* was successful expressed, purified and crystallized and X-ray diffraction data collection was performed. The calculation of the Matthews coefficient V_M (Matthews, 1968) as 2.9 Å^3 Da^{-1} with a corresponding solvent content of 58% for two monomers offers the most probable solution. The self-rotation function (Fig. 2) shows an independent noncrystallographic twofold axis. Based on the self-rotation function and the Matthews coefficient, we deduced the presence of a dimer in the asymmetric unit. The structure could be solved directly at the beamline using the SAS protocol of the automated crystal structure-determination platform *Auto-Rickshaw* (Panjikar *et al.*, 2005), which incorporates *SHELXC* (Sheldrick, 2001), *SHELXD* (Schneider & Sheldrick, 2002), *ABS* (Hao, 2004), *SHELXE* (Sheldrick, 2002) and *DM* (Cowtan, 1994). Automatic tracing using *ARP*/*wARP* (Perrakis *et al.*, 1999) yielded 97% of the polypeptide model and indeed shows

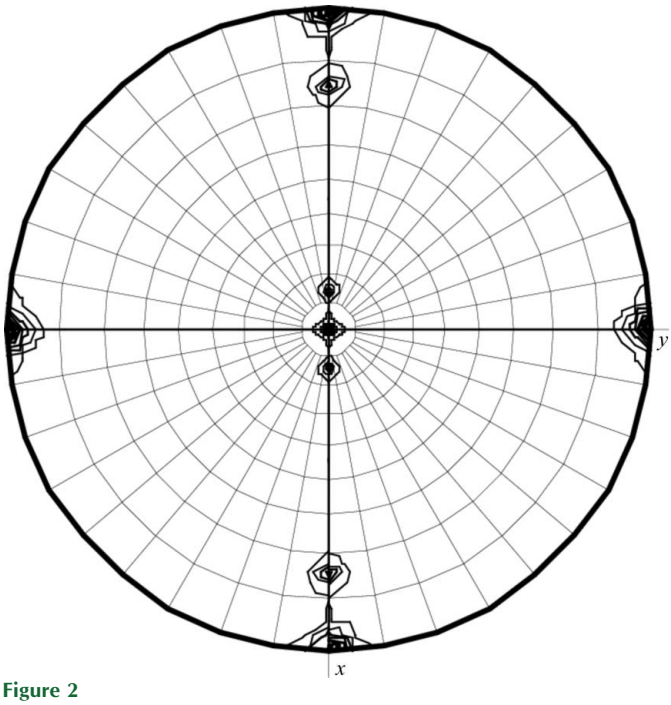

Figure 2
The self-rotation function at $\chi = 180^\circ$ for the diffraction data of (*R*)-selective amine transaminase from *A. fumigatus* in space group $C222_1$ reveals one independent twofold axis with noncrystallographic symmetry. In the orthorhombic space group the dyad-related monomers and their rotational symmetry mates display 16 noncrystallographic relationships including eight twofold axes. In the packing arrangement these axes coincide pairwise, causing four peaks (60% of the origin) in the self-rotation function at $\chi = 180^\circ$ with $\omega = 15$ or 75° and $\varphi = 0$ or 180°.

a dimer in the asymmetric unit. Currently, manual completion of the model and refinement against the high-resolution data is in progress.

Similarly to this amine transaminase, we have crystallized another (*R*)-selective amine transaminase from *Neosartorya fischeri* (96% sequence identity) from a concentrated protein solution without adding a specific precipitant.

MT thanks the Landesgraduiertenkolleg Mecklenburg-Vorpommern for financial support. We thank the European Union (KBBE-2011-5, grant No. 289350) for financial support within the European Union Seventh Framework Programme. Diffraction data were collected on BL14.1 operated by the Helmholtz-Zentrum Berlin (HZB) at the BESSY II electron-storage ring (Berlin-Adlershof, Germany).

References

Cowtan, K. (1994). *Jnt CCP4/ESF–EACBM Newsl. Protein Crystallogr.* **31**, 34–38.
Deng, L., Mikusová, K., Robuck, K. G., Scherman, M., Brennan, P. J. & McNeil, M. R. (1995). *Antimicrob. Agents Chemother.* **39**, 694–701.
Eliot, A. C. & Kirsch, J. F. (2004). *Annu. Rev. Biochem.* **73**, 383–415.
Han, Q., Robinson, H., Gao, Y. G., Vogelaar, N., Wilson, S. R., Rizzi, M. & Li, J. (2006). *J. Biol. Chem.* **281**, 37175–37182.
Hanson, K. R. (1966). *J. Am. Chem. Soc.* **88**, 2731–2742.
Hao, Q. (2004). *J. Appl. Cryst.* **37**, 498–499.
Hayashi, H. (1995). *J. Biochem.* **118**, 463–473.
Höhne, M. & Bornscheuer, U. T. (2009). *ChemCatChem*, **1**, 42–51.
Höhne, M. & Bornscheuer, U. T. (2012). *Enzymes in Organic Synthesis*, edited by W. Drauz, H. Gröger & O. May, pp. 779–820. Weinheim: Wiley-VCH.
Höhne, M., Schätzle, S., Jochens, H., Robins, K. & Bornscheuer, U. T. (2010). *Nature Chem. Biol.* **6**, 807–813.
Humble, M. S., Cassimjee, K. E., Håkansson, M., Kimbung, Y. R., Walse, B., Abedi, V., Federsel, H. J., Berglund, P. & Logan, D. T. (2012). *FEBS J.* **279**, 779–792.
Kabsch, W. (2010). *Acta Cryst.* D**66**, 125–132.
Karplus, P. A. & Diederichs, K. (2012). *Science*, **336**, 1030–1033.
Krug, M., Weiss, M. S., Heinemann, U. & Mueller, U. (2012). *J. Appl. Cryst.* **45**, 568–572.
Latgé, J.-P. (1999). *Clin. Microbiol. Rev.* **12**, 310–350.
Mani Tripathi, S. & Ramachandran, R. (2006). *J. Mol. Biol.* **362**, 877–886.
Martens, J., Günther, K. & Schickedanz, M. (1986). *Arch. Pharm.* **319**, 461–465.
Matthews, B. W. (1968). *J. Mol. Biol.* **33**, 491–497.
Merck (2001). *The Merck Index: An Encyclopaedia of Chemicals, Drugs and Biologicals*. Whitehouse Station: Merck Manuals.
Mueller, U., Darowski, N., Fuchs, M. R., Förster, R., Hellmig, M., Paithankar, K. S., Pühringer, S., Steffien, M., Zocher, G. & Weiss, M. S. (2012). *J. Synchrotron Rad.* **19**, 442–449.
Panjikar, S., Parthasarathy, V., Lamzin, V. S., Weiss, M. S. & Tucker, P. A. (2005). *Acta Cryst.* D**61**, 449–457.
Perrakis, A., Morris, R. & Lamzin, V. S. (1999). *Nature Struct. Biol.* **6**, 458–463.
Savile, C. K., Janey, J. M., Mundorff, E. C., Moore, J. C., Tam, S., Jarvis, W. R., Colbeck, J. C., Krebber, A., Fleitz, F. J., Brands, J., Devine, P. N., Huisman, G. W. & Hughes, G. J. (2010). *Science*, **329**, 305–309.
Schätzle, S., Höhne, M., Redestad, E., Robins, K. & Bornscheuer, U. T. (2009). *Anal. Chem.* **81**, 8244–8248.
Schneider, T. R. & Sheldrick, G. M. (2002). *Acta Cryst.* D**58**, 1772–1779.
Schwarzenbacher, R. *et al.* (2004). *Proteins*, **55**, 759–763.
Sheldrick, G. M. (2002). *Z. Kristallogr.* **217**, 644–650.
Sheldrick, G. M., Hauptman, H. A., Weeks, C. M., Miller, R. & Usón, I. (2001). *International Tables for Crystallography*, Vol. *F*, edited by M. G. Rossmann & E. Arnold, pp. 333–351. Dordrecht: Kluwer Academic Publishers.
Steffen-Munsberg, F., Vickers, C., Thontowi, A., Schätzle, S., Tumlirsch, T., Humble, M. S., Land, H., Berglund, P., Bornscheuer, U. T. & Höhne, M. (2013). *ChemCatChem*, **5**, 150–153.
Vagin, A. & Teplyakov, A. (2010). *Acta Cryst.* D**66**, 22–25.
Winn, M. D. *et al.* (2011). *Acta Cryst.* D**67**, 235–242.